Langmuir

ARTICLE

pubs.acs.org/Langmuir

Periodicity-Controlled Two-Dimensional Crystalline Colloidal Arrays

Jian-Tao Zhang, Luling Wang, Xing Chao, and Sanford A. Asher*

Department of Chemistry, University of Pittsburgh, Pittsburgh, Pennsylvania 15260, United States

Supporting Information

ABSTRACT: We developed a convenient and fast approach to preparing close-packed two-dimensional (2-D) particle arrays on mercury surfaces. Addition of cosolvents, such as alcohols, to aqueous colloidal particle suspensions induces spreading and self-assembly of the particles into 2-D arrays on top of the mercury surface. We can fabricate large-area close-packed 2-D arrays (>70 cm^2) within 30 s. We attached these 2-D arrays to functional hydrogel films such that the 2-D array spacings were altered by the hydrogel volume response to the environment. We directly observed the hydrogel volume induced 2-D array spacing changes by using confocal laser scanning microscopy to monitor the spacings of fluorescent polystyrene particle 2-D arrays in response to changes in pH, solvent composition, temperature, etc.

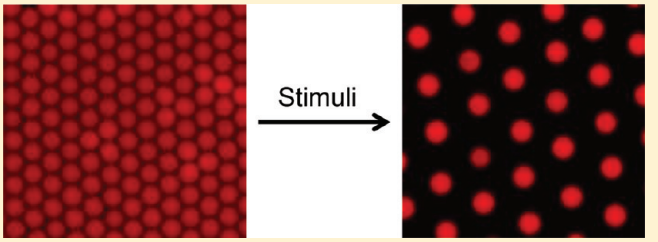

1. INTRODUCTION

Two-dimensional (2-D) monolayer crystalline colloidal arrays (CCAs) have been extensively investigated due to their applications in surface patterning and photonic materials.[1−4] Various 2-D arrays have been prepared by self-assembly of colloidal particles through solvent evaporation, spin-coating, and electric field driven assembly.[5−7] 2-D arrays have also been prepared at air−liquid interfaces.[8−13] These methods prepare hexagonally close-packed arrays. However, non-close-packed (ncp) arrays would be preferable in many applications, because they would allow their spacings to be both increased and decreased.[14,15] Additionally, ncp arrays could be used as lithographical masks to prepare, for example, tunable size nanopores.[16]

Various techniques have been developed to control 2-D crystal array lattice spacings.[9] 2-D ncp arrays have been prepared from 2-D close-packed colloidal crystals with plasma, reactive ion, and electron beam etching.[17,18] These methods require the use of expensive instrumentation, and the particle spacing is limited by the size of the colloidal particle template.[19] Yang and co-workers recently reported a soft lithography method to prepare 2-D ncp colloidal crystals with controllable lattice spacings and lattice structures.[19] They applied poly(dimethylsiloxane) (PDMS) elastomer stamps to the 2-D colloidal crystal films. After incubation at 100 °C for 3 h, the PDMS stamps were peeled off, and a single-layer 2-D colloidal crystal was transferred onto the PDMS surface. A subsequent solvent-induced swelling or mechanical stretching of the PDMS increased the ncp array spacing.[19,20]

Jiang et al. reported a simple spin-coating technique to fabricate monolayer ncp colloidal crystals. Dispersions of silica spheres in triacrylate monomers were spin-coated and polymerized to form 2-D colloidal crystal array−polymer nanocomposites. After removal of the triacrylate polymer matrix by oxygen plasma etching, ncp colloidal crystal arrays remained.[21,22] In this technique the concentration of the particle suspension and the spinning speed were carefully controlled. Although various fabrication techniques for ncp arrays have been developed, an inexpensive and fast method that easily and accurately controls the 2-D array particle spacing is still needed.

We recently demonstrated a method to fabricate high diffraction efficiency 2-D photonic crystals for chemical sensing applications.[23] We attached thin hydrogel films to close-packed 2-D polystyrene (PS) particle arrays prepared on Hg surfaces. The system changed volume in response to the presence of specific chemical species.[23] We here describe and discuss the 2-D colloidal particle array fast assembly mechanism on Hg. We controlled the ncp 2-D array particle spacing by attaching hydrogels that change volume in response to pH, solvent, temperature, etc. We also directly monitored the ncp 2-D array particle spacings to assess the impact of spacing alterations on the array ordering.

2. EXPERIMENTAL SECTION

2.1. Materials. Acrylamide (AAm), acrylic acid (AAc), *N*-isopropylacrylamide (NIPAAm), 2-hydroxyethyl methacrylate (HEMA), *N*,*N*′-methylenebisacrylamide (MBAAm), 2-hydroxy-1-[4-(2-hydroxyethoxy) phenyl]-2-methyl-1-propanone (Irgacure 2959), ethylene glycol dimethylacrylate (EGDMA), Hg, citric acid, and lead nitrate ($Pb(NO_3)_2$) were purchased from Sigma-Aldrich and were used as received. 4-(Acryloylamido)benzo-18-crown-6 (4AB18C6) was purchased from Acros Organics. Methanol, ethanol (EtOH), propanol, 2-propanol, 1-butanol, acetone, and dimethyl sulfoxide (DMSO) were purchased from J. T. Baker Inc. NaOH and HCl were purchased from Thermo Scientific Inc. PS particles with diameters of 90, 235, 490, and 580 nm were synthesized

Received: August 26, 2011
Revised: October 17, 2011
Published: October 18, 2011

Table 1. Compositions of PAAm Hydrogels

	composition				
label	AAm[a] (mL)	MBAAm[b]	AAc (μL)	4AB18C6[c] (mg)	Irgacure 2959[d] (μL)
P2C3A20	1	3	20		20
P2C2A20	1	2	20		20
P2C1A20	1	1	20		20
P2C0.5A20	1	0.5	20		20
P2C2A5	1	2	5		20
P2C2A10	1	2	10		20
P2C2A40	1	2	40		20
P2C1 18C6	1	1		10	40

[a] The concentration of AAm is 10 wt % in water. [b] Concentration of MBAAm (%) relative to AAm. [c] A 10 mg mass of 4AB18C6 dissolved in 20 μL of DMSO. [d] The concentration of Irgacure 2959 is 33% (w/v) in DMSO.

according to previously reported emulsion polymerization methods.[24,25] Fluorescent PS spheres with diameters of 0.5 and 2.17 μm were purchased from Sigma-Aldrich. Silica (SiO_2) particles of 110 nm diameter were obtained from Nissan Chemical America Corp. SiO_2 particles of 260 nm diameter were synthesized according to a previously reported method.[26]

2.2. Preparation of 2-D Arrays on the Hg Surface. Organic cosolvents were added to colloidal particle suspensions at different volume ratios, and the resultant dispersions were vortexed for 1 min. The colloid suspensions (10−50 μL) were layered onto the Hg surface (in a 10 cm diameter plastic Petri dish), on which the colloidal particles self-assembled into a 2-D array. To attach these 2-D arrays onto substrates for scanning electron microscopy (SEM) measurements, Scotch brand foam tape (St. Paul, MN) was placed onto the 2-D arrays. After 1 min, the tape was peeled from the Hg surface.

2.3. Preparation of 2-D Arrays on Hydrogel Films. We used commercial 2.17 μm PS particles to fabricate the 2-D arrays on hydrogels. A series of hydrogels were polymerized onto the 2-D arrays of these PS particles on Hg.[23] The hydrogel polymerization solution containing monomer(s), cross-linker, and initiator was carefully layered onto the 2-D array on Hg. A glass slide (60 mm × 24 mm × 0.12 mm) was lowered onto the solution covering the 2-D array. The polymerization was initiated by UV light (UVGL-55 hand-held UV lamp, UVP, Upland, CA). The glass slide with the attached hydrogel film and the 2-D array was lifted from the Hg surface. The 2-D array hydrogel was peeled from the glass slide and washed with water. The 2-D array AAm hydrogel films were synthesized with the compositions listed in Table 1. The 2-D array poly(hydroxyethyl methacrylate) (PHEMA) hydrogel was synthesized by UV polymerization of 600 μL of HEMA and 6 μL of EGDMA in 400 μL of water. To prepare the temperature-sensitive poly(*N*-isopropylacrylamide) (PNIPAAm) hydrogel with the 2-D array, 1 mL of a 10 wt % NIPAAm solution (containing 0.2 wt % MBAAm), 5 μL of AAc, and 20 μL of Irgacure 2959 (in DMSO, 33% (w/v)) were photopolymerized.

2.4. Characterization. The size and size distribution of particles were measured using transmission electron microscopy (TEM; FEI Morgagni 268). The ordering and morphology of the arrays were observed using SEM (Joel JSM6390LV) after sputter-coating a layer of Au. To investigate the 2-D array particles on hydrogels, confocal laser scanning microscopy (CLSM; Leica TCS SP5) was used to observe the particle ordering. The excitation wavelength was 514 nm; the emission wavelength ranged from 533 to 563 nm. The samples were equilibrated under different experimental conditions. For example, AAm/AAc 2-D array hydrogels were equilibrated in water or 0.01 M NaOH, the crown ether hydrogels were equilibrated in aqueous Pb^{2+} solutions, the PHEMA hydrogels were equilibrated at different EtOH/water concentrations, and the PNIPAAm hydrogels were equilibrated at different temperatures, before CLSM measurements.

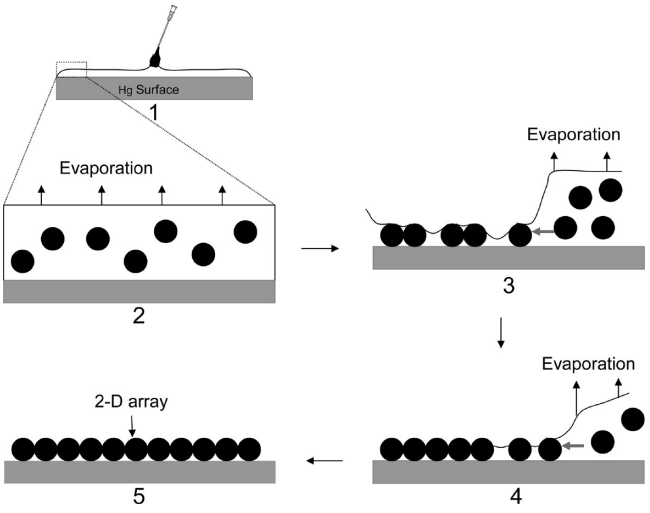

Figure 1. Illustration of the mechanism of 2-D particle array formation: (1) The particle suspension spreads on Hg to form a thin liquid film. (2) Solvents evaporate at the edge of the liquid film. (3, 4) A monolayer 2-D array forms at the edge due to solvent evaporation and suspension flows pushing the particles together. (5) A 2-D colloidal crystal array fills the entire Hg surface.

3. RESULTS AND DISCUSSION

3.1. Close-Packed 2-D Monolayer Arrays on the Hg Surface. We utilized Hg as a "liquid" substrate to enable the 2-D array formation. The Hg surface is molecularly smooth and mobile. The density of Hg is quite high (13.5 g·cm^{-3}), and it has a very high surface tension of 485 mN/m, causing the colloidal particle suspension to rapidly spread and self-assemble into a 2-D CCA on its surface.

A typical preparation of PS particle 2-D arrays on a Hg surface is shown in movie 1 (Supporting Information), where 20 μL of a 580 nm PS suspension containing 13.3 μL of a PS aqueous dispersion (20 wt %) and 6.7 μL of propanol was gradually and slowly layered onto a Hg surface. As shown in movie 1 and Figure 1, the 2-D colloidal crystal array formation occurs through flow-mediated self-assembly.[12,13,27,28] As the suspension spreads on Hg, the solvents evaporate. When the liquid film thickness becomes close to the particle diameter, the particles form 2-D array patches due to the lateral capillary forces that cause the particles to attract each other to form a close-packed 2-D hexagonal array on the Hg surface (Figure 1). The liquid suspension continues to flow from the thick center toward the outer edge of the 2-D array until a close-packed PS 2-D array monolayer fills the entire Hg surface. The preparation procedure is rapid and efficient. We obtain a >70 cm^2 2-D PS array in 30 s (see Figure S1 in the Supporting Information). Figure 2a shows the morphology of hexagonally close-packed 2-D arrays formed by 580 nm PS particles.

The fast formation of the 2-D PS crystal array is facilitated by propanol added to the suspension. Water has a surface tension of ~72.8 mN/m, while that of propanol is ~23.7 mN/m. The addition of propanol to the PS dispersion decreases the surface tension and increases the wetting ability of the Hg, causing the suspension to rapidly spread to form a thin film. The high vapor

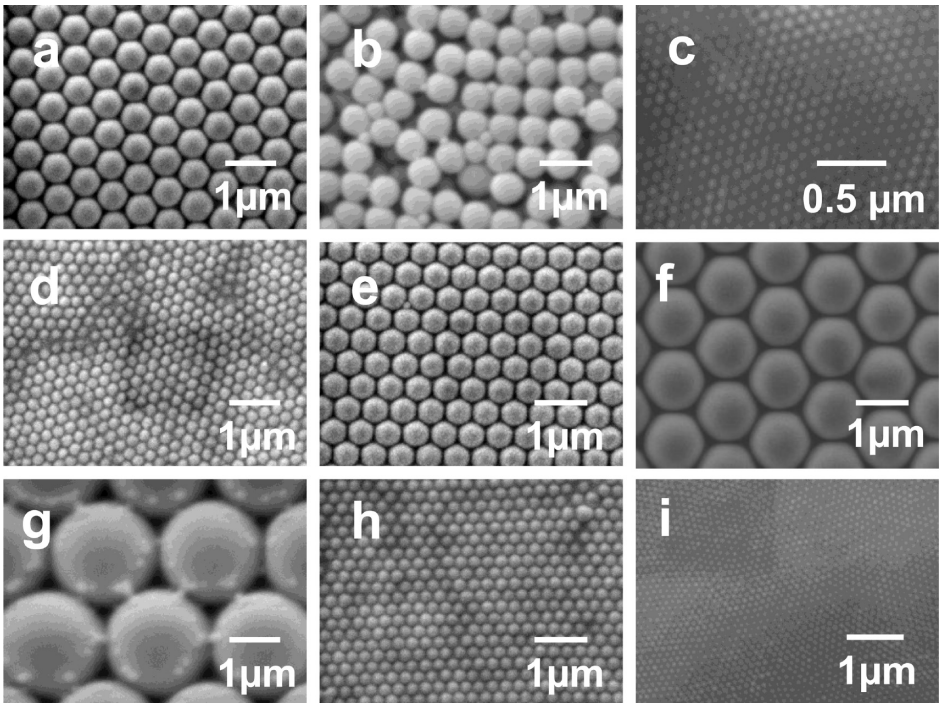

Figure 2. SEM images of 2-D arrays formed on a Hg surface: (a) 580 nm diameter PS array monolayer, (b) 580 nm diameter PS particle multilayer, (c−i) 2-D monolayers of (c) 90 nm diameter PS, (d) 235 nm diameter PS, (e) 490 nm diameter PS, (f) 1 μm diameter PS, (g) 2.17 μm diameter PS, (h) 260 nm diameter SiO_2, and (i) 110 nm diameter SiO_2. These arrays formed on Hg were transferred onto Scotch brand foam tape and were sputter-coated with Au for SEM measurements. The 2-D arrays in (a) and (c)−(i) were self-assembled by spreading water/propanol particle suspensions on Hg surfaces. The multilayer sample in (b) was prepared by spreading an aqueous PS suspension on a Hg surface, where a multilayer structure formed.

pressure of propanol also accelerates the spreading and speeds up the evaporation process, causing the rapid formation of 2-D arrays. The facile spreading and assembly of colloidal particles on Hg is not observed on rigid substrates, such as glass or silicon.

In contrast, aqueous PS dispersions without propanol spread slowly on Hg (Supporting Information, movie 2), forming multilayer structures as shown in Figure 2b. This results from the decreased wetting ability of the aqueous PS dispersion on Hg that limits the suspension spreading. We found that similar solvents such as methanol, ethanol, 2-propanol, butanol, and acetone can also be used to fabricate the PS array monolayers.

The PS particle concentration and the concentration of organic solvents can be widely varied. We obtain well-ordered and brightly diffracting 580 nm PS 2-D colloidal arrays (Figure S1, Supporting Information) on Hg with aqueous particle dispersion:propanol volume ratios from 3:1 to 1:3. By using a particle dispersion:propanol volume ratio of 2:1, we obtained excellent spreading and ordering for particle diameters between 90 nm and >2 μm (Figure 2c−g). Silica particle suspensions also spread to form hexagonally close-packed 2-D colloidal arrays on Hg (Figure 2h,i). The monolayer structure is definitively evident as shown in Figure S2 (Supporting Information). The 2-D colloidal crystals assembled on Hg surface are multidomain, with the largest single crystalline domain >1500 μm^2 in area (Figure S3, Supporting Information).

3.2. ncp 2-D Arrays. We used 2.17 μm fluorescent PS particles to fabricate 2-D arrays that we could easily study with CLSM. CLSM allows us to observe 2-D arrays in the wet state in air or in solution, in contrast to SEM, where the vacuum environment dehydrates the hydrogels. To examine our 2-D array spacing response to the chemical environment, we prepared a series of 2-D array hydrogels with the compositions listed in Table 1. We layered the polymerization solution containing the monomer(s), cross-linker, and initiator onto the 2-D array on Hg, lowered a glass slide onto the 2-D array polymerization solution, and then polymerized the hydrogel with UV light.

When the freshly prepared 2-D array hydrogel was immersed in water, it swelled, increasing the 2-D array spacing as shown by CLSM (Figure S4, Supporting Information). Most of the hydrogel reaches equilibrium within 1 h; however, we measured the spacing using CLSM over longer times (from several hours to overnight). For the close-packed P2C2A20 sample the center-to-center nearest neighbor spacing, d, was initially equal to the 2.17 μm PS particle diameter, d_0. The particle spacing increased to $(1.29 \pm 0.02)d_0$ upon equilibration with water. The ordering slightly degraded, as evident by the slight increase in the standard deviation of the particle spacing (Figure S4c,d).

3.2.1. Control of the ncp 2-D Array Spacing by Comonomers. Addition of AAc to the AAm hydrogels caused significant hydrogel swelling in basic solutions. Figure 3a shows the dependence of the 2-D array spacing on the AAc content in water and in 0.01 M aqueous NaOH solutions. In pure water, we observe similar nearest neighbor spacings of different AAc hydrogels ($\sim 1.25d_0$), because the carboxyl groups are primarily in their neutral COOH form. In contrast, in 0.01 M NaOH, the spacings increase with the amount of AAc added (Figure 3a). Addition of 5, 10, 20, and 40 μL of AAc gave 2-D array spacings of $1.83d_0$, $2.15d_0$, $2.69d_0$, and $2.91d_0$ in 0.01 M NaOH. Ionization of COOH results in a significantly increased Donnan potential, which swells the hydrogel and increases the 2-D particle spacings. The 2-D PS particle ordering remains hexagonal,

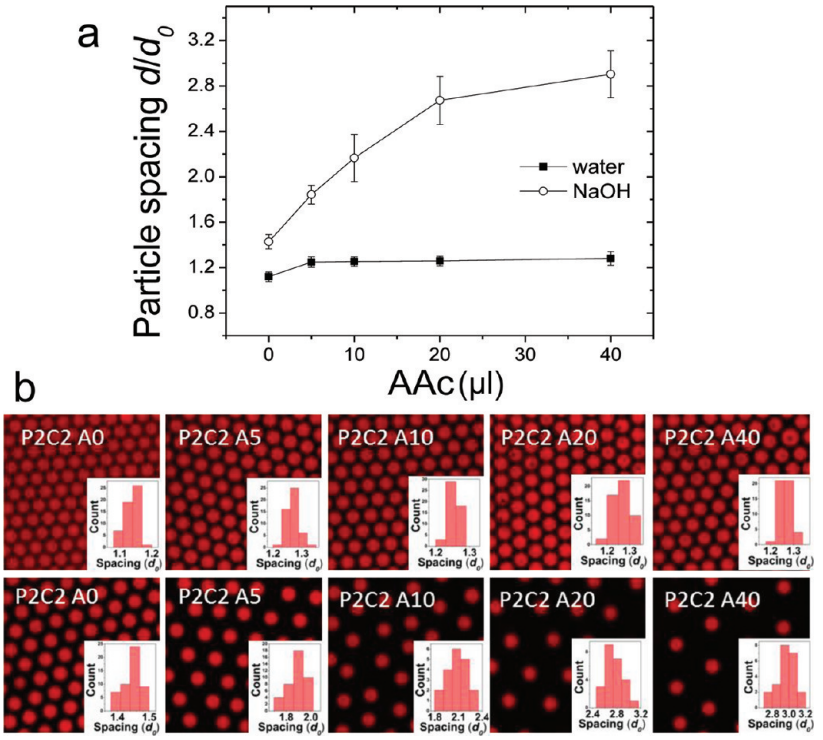

Figure 3. (a) Dependence of the 2-D array nearest neighbor particle spacing on added AAc. (b) CLSM images of 2-D arrays of P2C2A0, P2C2A5, P2C2A10, P2C2A2, and P2C2A40 hydrogels swollen in water (top images) and 0.01 M NaOH (bottom images). The insets show the nearest neighbor particle spacing distribution histograms.

but the ordering decreases somewhat with the softening of the gels as the hydrogels swell (Figure 3b). Some of the decreased ordering may result from deformations that are induced by sample handling.

3.2.2. Control of the ncp 2-D Array Spacing by the Cross-Link Density. As expected, the hydrogel swelling depends on the hydrogel cross-link density. The 2-D array spacing increases as the cross-link density decreases (Figure S5, Supporting Information). For example, the nearest neighbor spacing of P2C3A20 of $2.21d_0$ in 0.01 M NaOH increases to $2.66d_0$, $3.01d_0$, and $3.62d_0$ at lower cross-link densities of 2%, 1%, and 0.5%, respectively. This is because an increase in the level of cross-linking from P2C0.5A20 to P2C3A20 increases the elastic constant. According to the Flory theory, this will decrease the swelling and further decrease the 2-D particle spacing.

3.2.3. Pb^{2+} Spacing Control. We previously developed three-dimensional (3-D) and 2-D photonic crystal hydrogel Pb^{2+} sensors by covalently attaching crown ether groups to the hydrogel.[23,29] Figure 4 shows that the 2-D array spacing increases as the Pb^{2+} concentration increases from 0 to 5 mM. Binding of Pb^{2+} to the crown ether forms a polyelectrolyte hydrogel,[29,30] where the increased Donnan potential causes the hydrogel to swell. As the Pb^{2+} concentration increases to 10 mM, the spacing decreases to $1.49d_0$, because the crown ether groups become saturated, and further Pb^{2+} concentration increases lead to increased ionic strengths and decreased Donnan potentials, as previously observed.[23,29,30]

3.2.4. pH Spacing Control. We studied the pH dependence of the particle spacing of the hydrogel P2C2A20 that contains AAc. Figure 5 shows the dependence of the nearest neighbor 2-D array spacing between pH 2.75 and pH 7. We observe that the largest spacing changes occur around pH 4.3, the pK_a of the COOH

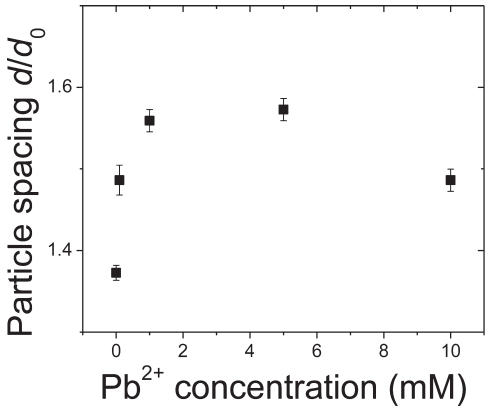

Figure 4. Dependence of the nearest neighbor 2-D particle spacing (d/d_0) on the Pb^{2+} concentration. P2C1 18C6 hydrogels were equilibrated in aqueous $Pb(NO_3)_2$ solutions.

groups. The spacing increases from $1.15d_0$ to $2.4d_0$ when the pH reaches the pK_a value. The formation of COO^- also results in an increased Donnan potential that causes hydrogel swelling.[31]

3.2.5. Ethanol Spacing Control. We previously showed that PHEMA 3-D polycrystalline colloidal array (PCCA) hydrogels swell in the presence of EtOH.[31b] Here we use EtOH to control the particle spacing of the PHEMA hydrogel 2-D arrays. Figure 6 shows the EtOH dependence of the particle spacing in a 2-D array HEMA hydrogel. d increases from $1.04d_0$ to $1.45d_0$ with increasing EtOH from 0 to 60−80 vol %. At the highest EtOH concentration, d decreases slightly to $1.3d_0$, indicating shrinking of the PHEMA hydrogel. These results agree well with a previous PHEMA hydrogel study.[32]

dx.doi.org/10.1021/la203363e |*Langmuir* 2011, 27, 15230–15235

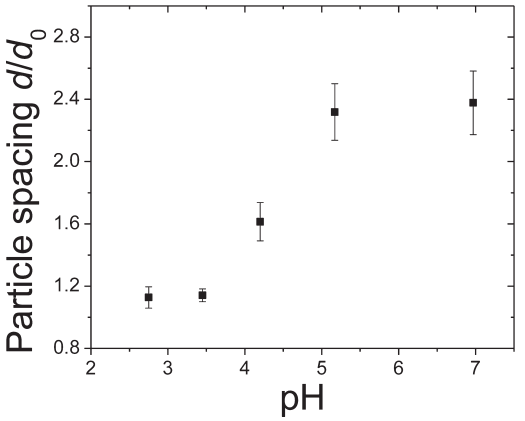

Figure 5. pH dependence of the 2-D PS array particle spacing (d/d_0) of P2C2A20 hydrogels equilibrated in citrate buffer solution (0.01 M) at different pH values.

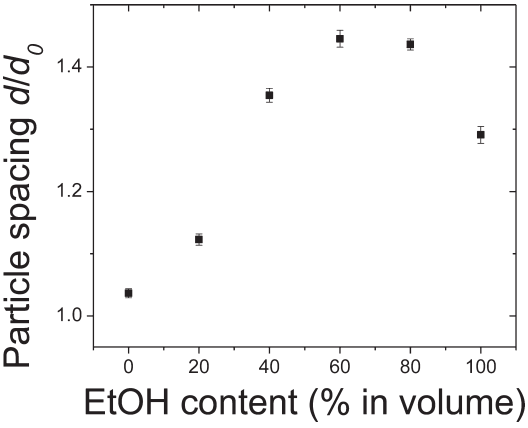

Figure 6. Dependence of the 2-D PS array particle spacing (d/d_0) of PHEMA hydrogels equilibrated in water/EtOH solutions.

The swelling of PHEMA in solvents depends on the hydrogel solubility parameter.[32−35] When the solvent solubility parameter (δ) is close to that of the polymer, the swelling of the hydrogel polymer, S, reaches a maximum value (S_{max}): $S/S_{max} = \exp[aS(\delta_s - \delta_p)^2]$, where a is a constant. δ_s and δ_p are the solubility parameters of the solvent and polymer network.

For a PHEMA hydrogel containing 1% EGDMA, δ_{PHEMA} is 29.6 $MPa^{1/2}$,[34] while water and EtOH have δ values of 47.8 and 26.5 $MPa^{1/2}$, respectively.[35] Increasing the EtOH content decreases $\delta_{solvent}$, increasing the hydrogel swelling. The highest swelling of PHEMA hydrogel should occur for an EtOH/water solution with a volume ratio of ~85:15. The hydrogel shrinkage that occurs at very high EtOH concentrations results from an increased difference in the solubility parameters between the solvent and the hydrogel polymer.

3.2.6. Temperature Spacing Control. PNIPAAm is an extensively studied temperature-sensitive polymer that shows a volume phase transition temperature of ~32 °C.[36] PNIPAAm materials have been used for drug delivery, photonic crystals, microlenses, etc.[37] Incorporation of hydrophilic monomers into PNIPAAm hydrogels generally increases the phase transition temperature.[38−40] We copolymerized 5 μL of AAc with 100 mg of NIPAAm. The resulting hydrogel showed a phase transition temperature of ~55 °C. Figure 7 shows the temperature dependence of the spacing d of a 2-D array on a PNIPAAm/AAc hydrogel. At 15 °C, the spacing d is $1.72d_0$. With increasing temperature, d gradually decreases. When the temperature is above 55 °C, d decreases to a value close to d_0 and the 2-D array becomes nearly close-packed. This process enables temperature control of the particle spacing.

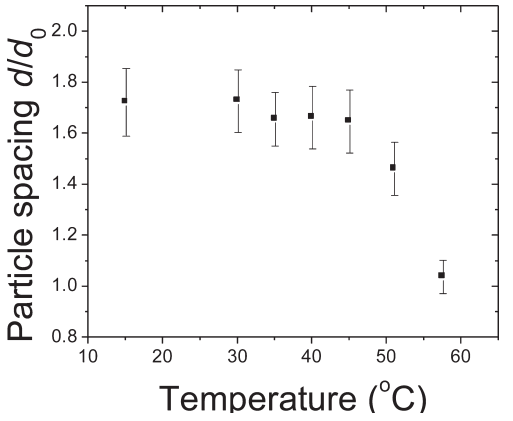

Figure 7. Temperature dependence of the 2-D PS array particle spacing (d/d_0) of PNIPAAm hydrogels. The samples are equilibrated for 24 h in water at each temperature.

3.3. Dehydration/Rehydration 2-D Array Cycling. Many hydrogels irreversibly collapse on dehydration, which limits their applications. For example, most 3-D PCCAs do not regain diffraction after rehydration due to irreversible changes in morphology and the collapse of the hydrogel.[41] In contrast, we observe reversible dehydration and rehydration of our 2-D PS array hydrogels. The 2-D array particle spacing d reversibly shrinks during dehydration in air and swells under rehydration in 0.01 M NaOH over multiple cycles (Figure S6, Supporting Information). This hydration/dehydration reversibility enables the long-term storage and transport of these 2-D hydrogel photonic crystals in their dry state.

4. CONCLUSIONS

We developed a facile approach to fabricate close-packed 2-D colloidal particle arrays by spreading PS particle dispersions on Hg surfaces. We attached these close-packed 2-D particle arrays onto functional hydrogel films. We can control the particle spacing, d, by changing the hydrogel environment, such as the pH, ion strength, solvent composition, and temperature.

■ ASSOCIATED CONTENT

Supporting Information. Movies of particle suspension spreading on Hg, photograph image of the 2-D array on Hg, SEM image of the edge of a 2-D array hydrogel, particle spacing data for the 2-D array with different cross-linker contents, and particle spacing of the 2-D array upon dehydration/rehydration cycling. This material is available free of charge via the Internet at http://pubs.acs.org/.

■ AUTHOR INFORMATION

Corresponding Author
*E-mail: asher@pitt.edu.

■ ACKNOWLEDGMENT

We gratefully acknowledge financial support from HDTRA (Grant 1-10-1-0044).

REFERENCES

(1) Xia, Y.; Gates, B.; Yin, Y.; Lu, Y. *Adv. Mater.* **2000**, *12*, 693–713.
(2) Galisteo−López, J. F.; Ibisate, M.; Sapienza, R.; Froufe−Pérez, L. S.; Blanco, A.; López, C. *Adv. Mater.* **2011**, *23*, 30–69.
(3) Li, F.; Josephson, D. P.; Stein, A. *Angew. Chem., Int. Ed.* **2011**, *50*, 360–388.
(4) Li, Y.; Koshizaki, N.; Cai, W. *Coord. Chem. Rev.* **2011**, *255*, 357–373.
(5) Kralchevsky, P. A.; Denkov, N. D. *Curr. Opin. Colloid Interface Sci.* **2001**, *6*, 383–401.
(6) Dejeu, J.; Bechelany, M.; Philippe, L.; Rougeot, P.; Michler, J.; Gauthier, M. *ACS Appl. Mater. Interfaces* **2010**, *2*, 1630–1636.
(7) Xie, R.; Liu, X. Y. *Adv. Funct. Mater.* **2008**, *18*, 802–809.
(8) Retsch, M.; Zhou, Z.; Rivera, S.; Kappl, M.; Zhao, X. S.; Jonas, U.; Li, Q. *Macromol. Chem. Phys.* **2009**, *210*, 230–241.
(9) Zhang, J.; Li, Y.; Zhang, X.; Yang, B. *Adv. Mater.* **2010**, *22*, 4249–4269.
(10) Li, C.; Hong, G.; Wang, P.; Yu, D.; Qi, L. *Chem. Mater.* **2009**, *21*, 891–897.
(11) Yoshimura, H.; Matsumoto, M.; Endoa, S.; Nagayama, K. *Ultramicroscopy* **1990**, *32*, 265–274.
(12) Yamaki, M.; Matsubara, K.; Nagayama, K. *Langmuir* **1993**, *9*, 3154–3158.
(13) Dimitrov, A. S.; Dushkin, C. D.; Yoshimura, H.; Nagayama, K. *Langmuir* **1994**, *10*, 432–440.
(14) Liu, Y.; Xie, R. G.; Liu, X. Y. *Appl. Phys. Lett.* **2007**, *91*, 063105−1–3.
(15) Jiang, P.; McFarland, M. J. *J. Am. Chem. Soc.* **2005**, *127*, 3710–3711.
(16) Haynes, C. L.; Van Duyne, R. P. *J. Phys. Chem. B* **2001**, *105*, 5599–5611.
(17) Plett, A.; Enderle, F.; Saitner, M.; Manzke, A.; Pfahler, C.; Wiedemann, S.; Ziemann, P. *Adv. Funct. Mater.* **2009**, *19*, 3279–3284.
(18) Tan, B. J. Y.; Sow, C. H.; Lim, K. Y.; Cheong, F. C.; Chong, G. L.; Wee, A. T. S.; Ong, C. K. J. *J. Phys. Chem. B* **2004**, *108*, 18575–19579.
(19) Li, X.; Wang, T.; Zhang, J.; Yan, X.; Zhang, X.; Zhu, D.; Li, W.; Zhang, X.; Yang, B. *Langmuir* **2010**, *26*, 2930–2936.
(20) Yan, X.; Yao, J. M.; Lu, G.; Li, X.; Zhang, J.; Han, K.; Yang, B. *J. Am. Chem. Soc.* **2005**, *127*, 7688–7689.
(21) Jiang, P.; Prasad, T.; McFarland, M. J.; Colvin, V. L. *Appl. Phys. Lett.* **2006**, *89*, 011908−1–3.
(22) Jiang, P.; McFarland, M. J. *J. Am. Chem. Soc.* **2004**, *126*, 13778–13786.
(23) Zhang, J. T.; Wang, L.; Luo, J.; Tikhonov, A.; Kornienko, N.; Asher, S. A. *J. Am. Chem. Soc.* **2011**, *133*, 9152–9155.
(24) Reese, C.; Asher, S. A. *J. Colloid Interface Sci.* **2002**, *248*, 41–46.
(25) Reese, C.; Guerrero, J.; Weissman, K. L.; Asher, S. A. *J. Colloid Interface Sci.* **2000**, *232*, 76–80.
(26) Stöber, W.; Fink, A.; Bohn, E. *J. Colloid Interface Sci.* **1968**, *26*, 62–69.
(27) Lazarov, G. S.; Denkov, N. D.; Velev, O. D.; Kralchevsky, P. A.; Nagayama, K. *J. Chem. Soc., Faraday Trans.* **1994**, *90*, 2077–2083.
(28) Nagayama, K.; Dimitrov, A. S. In *Film Formation in Waterborne Coatings*; Provderl, T., Winnik, M. A., Urban, M. W., Eds.; American Chemical Society: Washington, DC, 1996; pp 468−489.
(29) Reese, C.; Asher, S. A. *Anal. Chem.* **2003**, *75*, 3915–3918.
(30) Yan, F.; Asher, S. A. *Anal. Bioanal. Chem.* **2007**, *387*, 2121–2130.
(31) (a) Xia, X.; Hu, Z. *Langmuir* **2004**, *20*, 2094–2098. (b) Xu, X.; Goponenko, A. V.; Asher, S. A. *J. Am. Chem. Soc.* **2008**, *130*, 3113–3119. (c) Lee, Y. J.; Braun, P. V. *Adv. Mater.* **2003**, *15*, 563–566.
(32) Guvendiren, M.; Burdick, J. A.; Yang, S. *Soft Matter* **2010**, *6*, 5795–5801.
(33) Gee, G. In *Advances in Colloid Science*; Mark, H., Whitby, G. S., Meehan, E. J., Eds.; Interscience: New York, 1946; Vol. II, p 145.
(34) Caykara, T.; Ozyurek, C.; Kantoglu, O.; Guven, O. *J. Polym. Sci., Part B: Polym. Phys.* **2002**, *40*, 1995–2003.
(35) Barton, A. F. M. *Chem. Rev.* **1975**, *75*, 731–753.
(36) (a) Heskins, M.; Guillet, J. E. *J. Macromol. Sci., Chem.* **1968**, *2*, 1441–1455. (b) Ahmed, Z.; Gooding, E. A.; Pimenov, K. V.; Wang, L.; Asher, S. A. *J. Phys. Chem. B* **2009**, *113*, 4248–4256. (c) Zhang, J. T.; Jandt, K. D. *Macromol. Rapid Commun.* **2008**, *29*, 593–597. (d) Hu, Z.; Lu, X.; Gao, J. *Adv. Mater.* **2001**, *13*, 1708–1712. (e) Takeoka, Y.; Watanabe, M. *Adv. Mater.* **2003**, *15*, 199–201.
(37) (a) Rzaev, Z. M. O.; Dinçer, S.; Pişkin, E. *Prog. Polym. Sci.* **2007**, *32*, 534–595. (b) Nolan, C. M.; Gelbaum, L. T.; Lyon, L. A. *Biomacromolecules* **2006**, *7*, 2918–2922. (c) Zhang, J. T.; Xue, Y. N.; Gao, F. Z.; Huang, S. W.; Zhuo, R. X. *J. Appl. Polym. Sci.* **2008**, *108*, 3031–3037. (d) Zhang, J. T.; Huang, S. W.; Zhuo, R. X. *Colloid Polym. Sci.* **2005**, *284*, 209–213. (e) Huang, G.; Hu, Z. *Macromolecules* **2007**, *40*, 3749–3756. (f) Kim, J.; Nayak, S.; Lyon, L. A. *J. Am. Chem. Soc.* **2005**, *127*, 9588–9592. (g) Reese, C. E.; Mikhonin, A. V.; Kamenjicki, M.; Tikhonov, A.; Asher, S. A. *J. Am. Chem. Soc.* **2004**, *126*, 1493–1496. (h) Weissman, J. M.; Sunkara, H. B.; Tse, A. S.; Asher, S. A. *Science* **1996**, *274*, 959–960. (i) Zhang, J. T.; Keller, T. F.; Bhat, R.; Garipcan, B.; Jandt, K. D. *Acta Biomater.* **2010**, *6*, 3890–3898.
(38) Shibayama, M.; Mizutani, S.; Nomura, S. *Macromolecules* **1996**, *29*, 2019–2024.
(39) Feil, H.; Bae, Y. H.; Feijen, J.; Kim, S. W. *Macromolecules* **1993**, *26*, 2496–2500.
(40) Otake, K.; Inomata, H.; Konno, M.; Saito, S. *Macromolecules* **1990**, *23*, 283–289.
(41) Muscatello, M. M. W.; Asher, S. A. *Adv. Funct. Mater.* **2008**, *18*, 1186–1193.